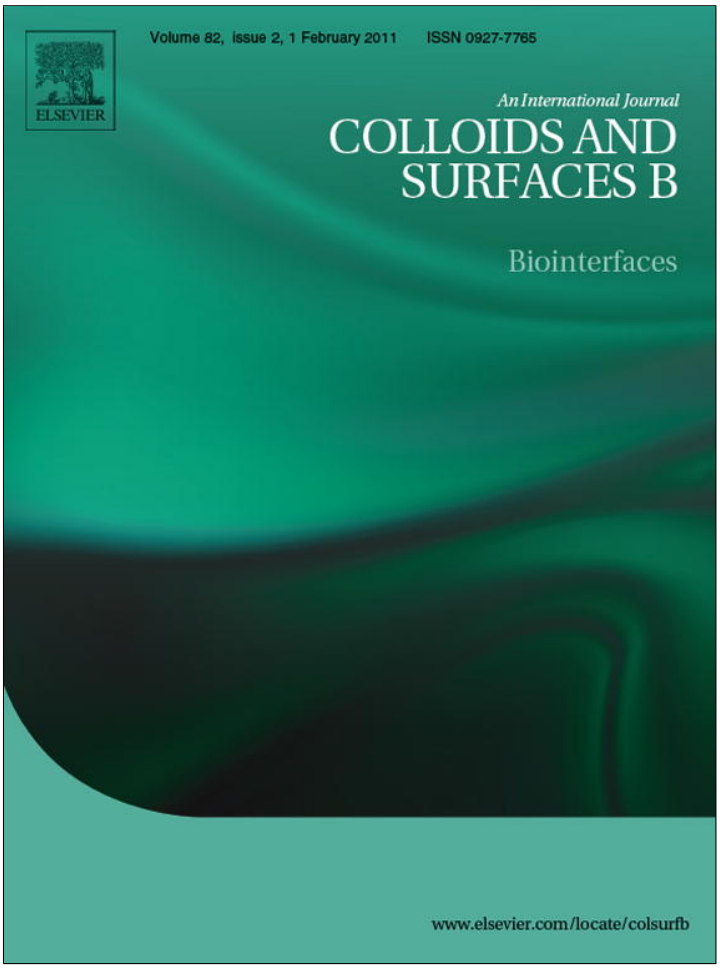

Colloids and Surfaces B: Biointerfaces 82 (2011) 307–315

Contents lists available at ScienceDirect

Colloids and Surfaces B: Biointerfaces

journal homepage: www.elsevier.com/locate/colsurfb

Electrospun collagen–chitosan–TPU nanofibrous scaffolds for tissue engineered tubular grafts

Chen Huang[a,b], Rui Chen[a,b], Qinfei Ke[a,b], Yosry Morsi[c], Kuihua Zhang[a,d], Xiumei Mo[a,*]

[a] Key Laboratory of Textile Science & Technology, Ministry of Education, Donghua University, Shanghai 201620, China
[b] College of Textiles, Donghua University, Shanghai 201620, China
[c] Faculty of Engineering and Industry Science, Swinburne University of Technology, Melbourne, Victoria 3122, Australia
[d] College of Biological Engineering and Chemical Engineering, Jiaxing College, Zhejiang 314001, China

ARTICLE INFO

Article history:
Received 30 July 2010
Received in revised form 26 August 2010
Accepted 1 September 2010
Available online 15 September 2010

Key words:
Electrospun
Collagen–chitosan–TPU
Nanofibrous scaffolds
Cell morphology
Tissue engineering

ABSTRACT

The objective of this study is to design a novel kind of scaffolds for blood vessel and nerve repairs. Random and aligned nanofibrous scaffolds based on collagen–chitosan–thermoplastic polyurethane (TPU) blends were electrospun to mimic the componential and structural aspects of the native extracellular matrix, while an optimal proportion was found to keep the balance between biocompatibility and mechanical strength. The scaffolds were crosslinked by glutaraldehyde (GTA) vapor to prevent them from being dissolved in the culture medium. Fiber morphology was characterized using scanning electron microscopy (SEM) and atomic-force microscopy (AFM). Fourier transform infrared spectroscopy (FTIR) showed that the three-material system exhibits no significant differences before and after crosslinking, whereas pore size of crosslinked scaffolds decreased drastically. The mechanical properties of the scaffolds were found to be flexible with a high tensile strength. Cell viability studies with endothelial cells and Schwann cells demonstrated that the blended nanofibrous scaffolds formed by electrospinning process had good biocompatibility and aligned fibers could regulate cell morphology by inducing cell orientation. Vascular grafts and nerve conduits were electrospun or sutured based on the nanofibrous scaffolds and the results indicated that collagen–chitosan–TPU blended nanofibrous scaffolds might be a potential candidate for vascular repair and nerve regeneration.

1. Introduction

Autologous vein and artery segments have been claimed as the gold substitution for the repair of diseased vessels and peripheral nerve [1–3]. While vascular and nerve-related diseases can occur at any age in males and females, they become increasingly common as people get older. In those cases, the use of prosthetic vascular grafts can be offered as alternatives, as suitable autologous substitutions are probably not available. Tissue engineered grafts have been proposed as a promising solution, which involves the incorporation of isolated living cells from patients into three-dimensional scaffolds, followed by the transplantation of this scaffold back into the patient via surgery.

As a recently developed technology, tissue engineering is a multidisciplinary subject that combines genetic engineering of cells with chemical engineering to create artificial organs and tissues, such as skin, bones, blood vessels and nerve conduits [4]. The main challenge for tissue engineered scaffolds is to design and fabricate customizable biodegradable matrices that can mimic the componential and structural aspects of extracellular matrices (ECM) [5]. Native ECM include the interstitial matrix and the basement membrane. Gels of polysaccharides and fibrous proteins (collagen in particular) fill the interstitial space and act as a compression buffer against the stress placed on the ECM. Basement membranes are sheet-like depositions of ECM on which various epithelial cells rest [6]. Based on these facts, this study selected collagen as the protein part and chitosan as the polysaccharide part to fabricate ideal tissue engineered scaffolds.

As the main protein of connective tissue in animals and the most abundant protein in mammals [7], collagen is widely used as biomaterials in wound dressing and medical fields. Chitosan, a massive natural polysaccharide derived from chitin, could be used to replace glycosaminoglycan, which is the main component of natural ECM [8]. Both collagen and chitosan possess good biocompatibility, appropriate biodegradability and commercial availability. Various studies have found that collagen–chitosan complex might be an excellent candidate for tissue engineering due to its good cell viability [8–10]. However, there remains a non-ignorable gap between

* Corresponding author at: Biomaterials and Tissue Engineering, Donghua University, 2999 Renmin Rd. North, Songjiang District, Shanghai 20160, China. Tel.: +86 21 67792653; fax: +86 21 67792653.
E-mail addresses: xmm@dhu.edu.cn, med@dhu.edu.cn (X. Mo).

0927-7765/$ – see front matter © 2010 Elsevier B.V. All rights reserved.
doi:10.1016/j.colsurfb.2010.09.002

lab activities and clinical trials for the application of this type of complex, as the two materials are both too fragile to provide sufficient mechanical strength, which is indispensable for a successful tubular scaffold. Therefore, thermoplastic polyurethane (TPU) would be a good candidate for reinforcement. As a thermalplastic elastomer, TPU has been widely used as coating materials for breast implants, catheters, and prosthetic heart valve leaflets because of its supreme mechanical properties [11]. Although conventional TPUs are not intended to degrade, they are susceptible to hydrolytic, oxidative and enzymatic degradation in vivo.

In native ECM, interstitial matrix is presented as a three-dimensional structure formed by nanofibers. To architecturally mimic that structure, electrospinning technique was used because electrospun nanofiber matrices are characterized by ultrafine continuous fibers; high surface-to-volume ratio; high porosity and variable pore-size distribution, all of which are morphologically similar to the natural ECM [12]. As a simple but productive method, in recent years electrospinning technique has been widely used in biomedical fields for the production of both nonwoven and regulated matrixes [13–18].

Electrospinning technique provides a simple way to obtain nanofibers from both synthetic polymers and natural materials with the potential for tissue regeneration and repair. Collagen–chitosan electrospun complex and their biocompatibility have been reported previously [8,19], however, so far the scaffolds have not been successfully applied in blood vessel and nerve repair due to the mechanical limitation of natural materials. To overcome the problem, optimal ratio of collagen/chitosan/TPU has been selected to obtain a compromise between biocompatibility and mechanical strength in the present study. Glutaraldehyde (GTA) vapor crosslinking has been conducted to prevent collagen and chitosan from being dissolved in the water. Endothelial cells and Schwann cells were then seeded on the scaffolds to examine if the three-material based scaffold could be a suitable candidate for blood vessels and nerve repair. The orientation of electrospun nanofibers plays an important role in cell growth and related functions [20–24]. Therefore, aligned nanofibrous scaffolds were prepared to regulate cell morphology in this study. SEM and hematoxylin and eosin (H&E) staining images of cultured scaffolds demonstrated that both endothelial cells and Schwann cells have the propensity to grow along the direction of fiber alignment to some extent. Mechanical measurements of random and aligned fibrous matrices indicated that the limitation of natural materials could be solved by adding a low proportion of TPU into the mixture and such type of electrospun fibrous matrices might be a novel biomimetic tissue engineered scaffold in vessel and nerve repair.

2. Materials and methods

2.1. Materials

Collagen I (mol. wt., $0.8–1 \times 10^5$ Da) was purchased from Sichuan Ming-rang Bio-Tech Co. Ltd. (China), chitosan (85%, deacetylated, $M_\eta \approx 10^6$) was purchased from Ji-nan Haidebei Marine Bioengineering Co., Ltd. (China) and TPU polymer (Tecoflex EG-80A) was purchased from Noveon, Inc. (USA). 1,1,1,3,3,3-Hexafluoroisopropanol (HFP) from Fluorochem Ltd. (UK) and trifluoroacetic acid (TFA) from Sinopharm Chemical Reagent Co., Ltd. (China) were used to dissolve the collagen, chitosan, TPU and their blends. A crosslinking agent of aqueous glutaraldehyde (GTA) solution (25%) was purchased from Sinopharm Chemical Reagent Co., Ltd. (China). Porcine iliac artery endothelial cells (PIECs) and Schwann cells (SCs) were obtained from the Institute of Biochemistry and Cell Biology (Chinese Academy of Sciences, China). All culture media and reagents were purchased from Gibco Life Technologies Co., USA unless specified.

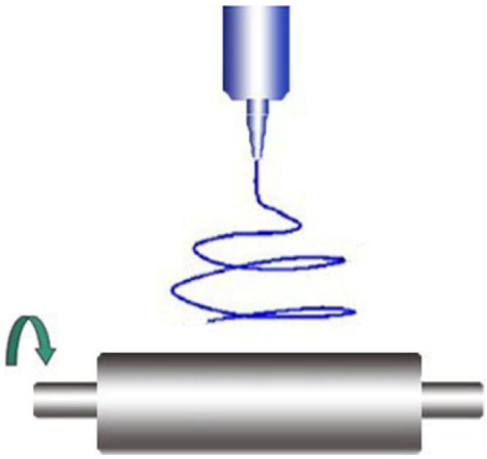

Fig. 1. Schematic diagram of electrospinning spinneret and rotating drum.

2.2. Electrospinning of collagen–chitosan–TPU scaffolds

Collagen (8 wt%) and TPU (6 wt%) were dissolved in HFP while chitosan (8 wt%) was dissolved in HFP/TFA mixture (v/v, 90/10). Before electrospinning, the three solutions were blended at a weight ratio of collagen/chitosan/TPU = 60%/15%/25% with sufficient stirring at room temperature for 1 h. The solutions were then filled into a 2.5 ml plastic syringe with a blunt-ended needle. The syringe was attached to a syringe pump (789100C, Cole-Pamer, America) and dispensed at a rate of 1.0 ml/h. A voltage of 18 kV was obtained from a high voltage power supply (BGG6-358, BMEI Co. Ltd., China) and applied across the needle and ground collector. Random nanofibers were collected on a flat collector plate wrapped with aluminum foil at a distance of 12–15 cm. Aligned nanofibers were formed on a rotating drum with a 6 cm diameter, rotation speed of 4000 r/min and 12 cm away from the tip of the syringe (Fig. 1). To compare orientation degree, pure TPU nanofibers were electrospun using the same parameters as above.

2.3. GTA vapor crosslinking

The crosslinking process was carried out by placing the collagen–chitosan–TPU nanofibrous membrane in a sealed, dual-layered desiccator containing 10 ml of 25% glutaraldehyde aqueous solution in a Petri dish. The membranes were fixed on a glass frame and were crosslinked in an atmosphere of water and glutaraldehyde vapor at room temperature for 2 days. The Petri dish was placed inside the bottom layer of the desiccator, while the nanofibrous membrane was fixed on a glass frame in the upper layer, above the semi-permeable divider. After crosslinking, samples were exposed in the vacuum oven at normal room temperature.

2.4. Characterization

Fiber morphology was observed with a scanning electronic microscope (SEM) (JSM-5600, Japan) at an accelerated voltage of 10 kV. The fibers were coated with gold sputter. Fiber diameters were estimated using image analysis software (ImageJ, National Institutes of Health, USA) and calculated by selecting 100 fibers randomly observed on the SEM images. A two-dimensional fast Fourier transform (2D FFT) approach [25] was adapted to measure fiber alignment in electrospun matrix. Surface properties of the nanofibers were examined using a nanoscope atomic-force microscope (Nanoscope IV, America), in the tapping mode and expressed as height and phase images.

Fourier transform infrared spectroscopy (FTIR) studies were carried out on compressed films containing KBr pellets and samples using a FTIR spectrophotometer (Avatar380, USA). All spectra were recorded in absorption mode at 2 cm^{-1} interval and in the wavelength range 4000–600 cm^{-1}.

The tensile strength test was performed on various electrospun collagen–chitosan–TPU specimens ($n = 6$ for each group) with random, parallel or perpendicular fiber alignment. All samples were of same size (30 mm × 10 mm), and the test was performed using a universal materials tester (H5 K-S, Hounsfield, UK) with a 50 N load cell at ambient temperature of 20 °C and humidity of 65%. A cross-head speed of 10 mm/min was used for all the specimens tested.

Electrospun nanofibrous scaffolds were cut into 30 mm × 30 mm squares for porometry measurement. A CFP-1100-AI capillary flow porometer (PMI Porous Materials Int.) was used in this study to measure pore size and pore distribution. Calwick with a surface tension of 21 dyn/cm (PMI Porous Materials Int.) was used as the wetting agent for porometry measurements. For each group, the test was repeated 3 times to gain a better accuracy.

2.5. Viability and morphology studies of PIECs and SCs

Porcine iliac artery endothelial cells and Schwann cells were cultured, respectively in Dulbecco's modified Eagle's medium (DMEM) and DMEM/F12 1:1 mixture medium with 10% fetal bovine serum and 1% antibiotic–antimycotic at an atmosphere of 5% CO_2 and 37 °C. The medium was replenished every 3 days. Electrospun scaffolds were prepared on circular glass coverslips (14 mm in diameter), which were then placed into the wells on a 24-well plate individually, and being secured with stainless rings. Before seeding cells, scaffolds were sterilized by immersion in 75% ethanol for 2 h, washed 3 times with phosphate-buffered saline solution (PBS), and then washed with culture medium. Cells were then seeded at a density of 1.0×10^4 cells/well of 24-well plates and tissue culture polystyrene (TCP) wells were seeded as control.

Cell viability on electrospun scaffolds was determined by methylthiazol tetrazolium (MTT) assay ($n = 6$ for each essay). After 1, 3, 5 and 7 days of cell seeding, the cells and matrices were incubated with 5 mg/ml 3-[4,5-dimethyl-2-thiazolyl]-2,5-diphenyl-2H-tetrazolium bromide (MTT) for 4 h. Thereafter, the culture media were extracted and 400 μl MTT were added for about 20 min. When the crystal was sufficiently dissolved, aliquots were pipetted into the wells of a 96-well plate and tested by an Enzyme-labeled Instrument (MK3, Thermo, USA), and the UV absorbance at 490 nm for each well was measured.

Cell morphology was examined by SEM after 3 days of culturing. The scaffolds were rinsed twice with PBS and fixed in 4% glutaraldehyde aqueous solution at 4 °C for 2 h. Fixed samples were rinsed twice with PBS and then dehydrated in gradient concentrations of ethanol (30%, 50%, 70%, 80%, 90%, 95% and 100%). After being dried in vacuum oven overnight, the cellular constructs were coated with gold sputter and observed under the SEM at a voltage of 10 kV. Hematoxylin and eosin (H&E) staining was also conducted on thinner scaffolds (thickness ≤100 μm) as complements to observe cell morphology.

3. Results and discussion

3.1. Morphology of electrospun fibers

It is generally accepted that nanofiber diameter, surface morphology and pore-size distribution could be affected apparently by electrospinning parameters including needle size, working distance, applied voltage, flow rate and working environment. To investigate the morphology of electrospun fibers, SEM micrographs of randomly oriented and aligned collagen–chitosan–TPU nanofibrous scaffolds were acquired with fiber diameter in the range of 360 ± 220 and 256 ± 145 nm, respectively (Fig. 2A and B). The reason why aligned nanofibers have a comparatively lower average diameter than that of randomly oriented nanofibers is probably because with such a high rotating speed, fibers are stretched and thus attenuated as soon as they reached the rotating collector. When the scaffolds were amplified to magnification ×10,000, many superfine fibers (diameter ≤100 nm) can be observed from Fig. 2C (pointed by the arrows) and the existence of these fibers could be explained by the positive charges carried by chitosan, which makes the mixture solution a more complicated system. These increased charges would increase solution conductivity and since the force that causes the stretching of the solution could be ascribed to the repulsive forces between the charges on the electrospinning jet, the stretching process would be enhanced owning to the increase of solution conductivity.

To observe the surface morphologies of collagen–chitosan–TPU nanofibers, atomic-force microscopy (AFM) was employed by using height mode (Fig. 3). It was reported that the surface of electrospun collagen fibers was comparatively rougher than that of electrospun synthetic polymers [26], whereas from our AFM images, with a TPU proportion of 25% it could be clearly observed that the surface of collagen–chitosan–TPU nanofibers was quite smooth and a groove on the right side of the fiber could be found. This phenomenon might be attributed to the complexity of mixture solution while the grooves were not found on all the fibers. From surface morphology images we can see that TPU component could improve the spinnability of polymer solution while the existence of grooves on some nanofibers would be conducive to cell adhesion and proliferation by providing adhesion sites for cell growth.

With the aim of measuring fiber alignment, a two-dimensional fast Fourier transform (2D FFT) approach described by Ayres et al. [25] was adapted. In brief, a quadrate region was captured from SEM images (Fig. 4A and B) and then analyzed with ImageJ software to create corresponding frequency plots and 2D FFT alignment plots. The two peaks at 175° and 355° in Fig. 4E show that with a rotation speed of 4000 r/min, pure TPU nanofibers were highly arrayed along one direction, however, in the three-material based system (Fig. 4F), fiber orientation could not be regulated with such a high uniformity. Although two main peaks could also be found at 5° and 185°, the existence of other peaks indicates that some nanofibers are not well aligned. This phenomenon demonstrates that besides ambient parameters such as applied voltage and rotating speed, properties of mixture solution (difference in molecular weight and electric-charge number) also play an indispensable role in the determination of fiber morphology.

3.2. Fourier transform infrared spectroscopy

In a complicated system containing three types of materials, the Fourier transform infrared spectroscopy (FTIR) could be used as an effective method to define the existence of each component. FTIR spectra of electrospun collagen–chitosan and collagen–TPU nanofibers were studied in previous work [8,26]. Fig. 5 depicted the FTIR spectra of non-crosslinked (Fig. 5a) and crosslinked (Fig. 5b) collagen–chitosan–TPU fibers with a weight ratio of 60%:15%:25% (collagen:chitosan:TPU).

As shown in Fig. 5a, the characteristic absorption bands of collagen were observed at 1650 cm^{-1} (amide I), 1530 cm^{-1} (amide II), 1200 cm^{-1} (amide III), respectively while the peak at 1130 cm^{-1} was assigned to chitosan for its saccharine structure. N–H and C–H stretches at 2940 cm^{-1} and 3300 cm^{-1} and other peaks overlapped with collagen between 1530 cm^{-1} and 1200 cm^{-1} were characteristic of TPU. Compared to Fig. 5a, Fig. 5b showed no sig-

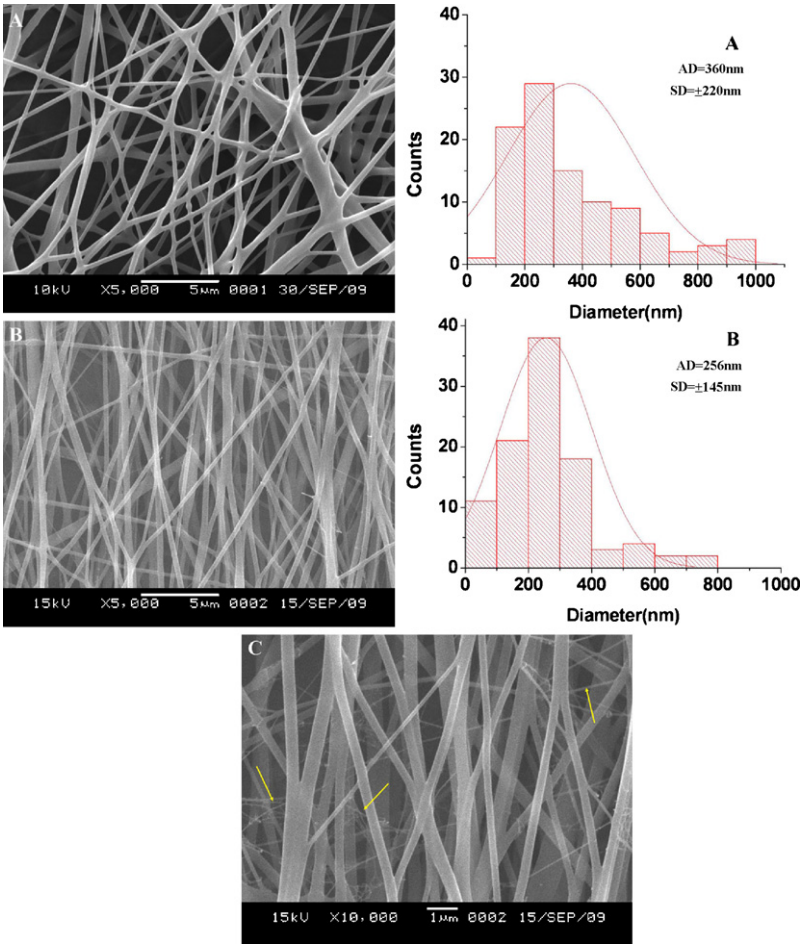

Fig. 2. SEM micrographs of collagen–chitosan–TPU nanofibers and their diameter distribution: (A) random oriented nanofibers; (B) and (C) aligned nanofibers with 5000 and 10,000 magnification.

nificant difference in the location of these characteristic peaks, this is probably because the absorption peak of –C=N– stretching vibration generated by GTA crosslinking could be in the range of 1640–1690 cm^{-1} and an overlap might have occurred with the strong absorption of the amide I band.

3.3. Pore size

For tissue engineered scaffolds, microscale and nanoscale porous structure are most favorable because the highly porous network of interconnected pores helps to facilitate the passage of nutrients and the exchange of gases, which are crucial for cellular growth and tissue regeneration [13]. Pore size and pore distribution analyses were conducted by automated capillary flow porometer system software and the results are shown in Table 1. It could be seen that when scaffolds were similar in thickness, the mean, largest and smallest pore diameter of randomly oriented collagen–chitosan–TPU nanofibrous scaffold were all larger than the corresponding measurements of aligned. This implies that parallel alignment can decrease pore size and lead a more evenly

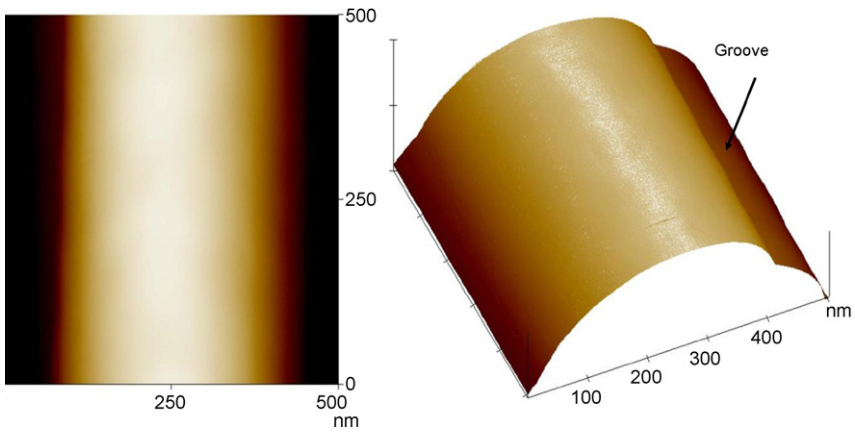

Fig. 3. AFM images represented by height model.

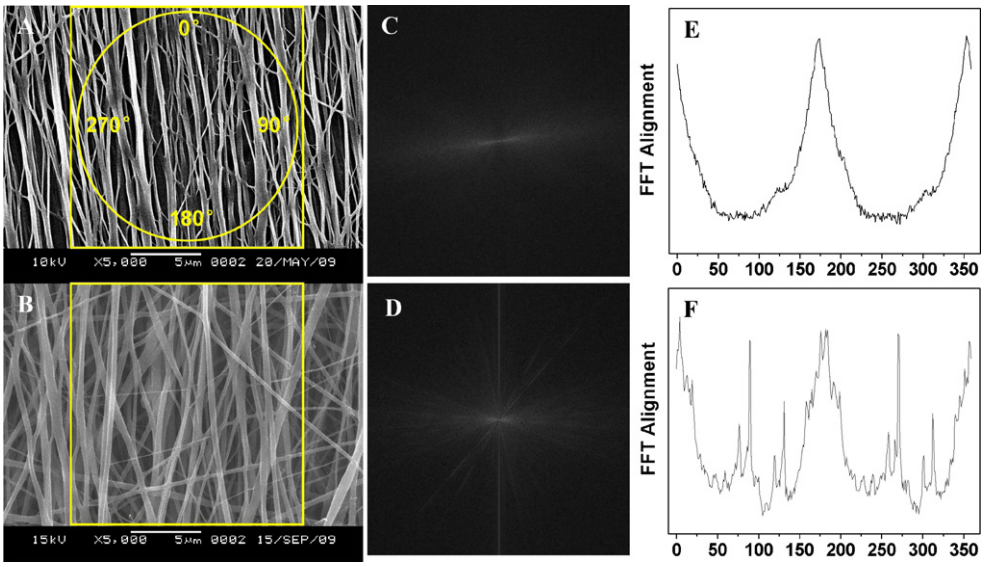

Fig. 4. SEM images of aligned electrospun scaffolds with a rotation speed of 4000 r/min ((A) represents pure TPU nanofibers while (B) represents collagen–chitosan–TPU nanofibers). ImageJ frequency plots (C and D) and 2D FFT alignment plots (E and F) for the corresponding quadrate regions.

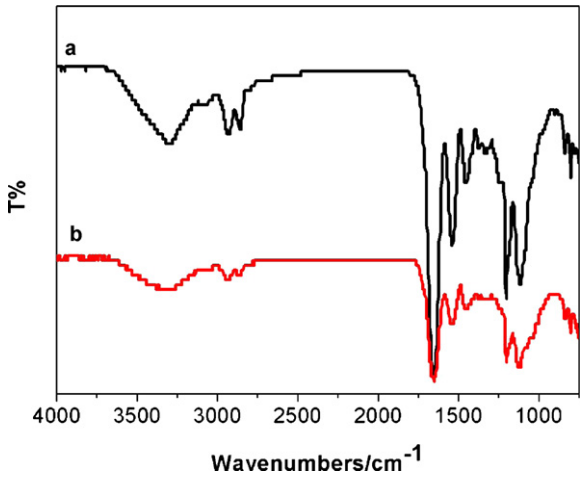

Fig. 5. FTIR spectra of coaxial collagen–chitosan–TPU electrospun nanofibrous membranes. Non-crosslinked (a); crosslinked (b).

pore-size distribution. What is more, we can conclude that after GTA vapor crosslinking, nanofibrous scaffolds become more compact because specimen thickness and pore size of both random and aligned scaffolds decreased dramatically.

3.4. Mechanical properties analysis

In the fabrication of tubular scaffolds, mechanical strength is of vital importance to provide enough support and this is the reason why natural materials, such as collagen and chitosan could not be used as the dominant component for electrospun grafts. It is reported that the tensile strength of a native artery is about 1.5 MPa [1], however, for scaffolds made from natural materials, a much higher strength is necessary when aspects like degradation and wet-strength loss are taken into consideration.

The typical tensile stress–strain curves of random oriented and aligned collagen–chitosan–TPU nanofibrous scaffolds (non-crosslinked, crosslinked) are shown in Fig. 6 while the average elongation at break and average tensile strength of each specimen are summarized in Table 2. Comparing Fig. 6A–C with Fig. 6A′–C′, it can be seen that GTA vapor crosslinking had a positive influence on tensile strength but a negative influence on average elongation at break. After crosslinking both randomly oriented and aligned scaffolds were tended to be more stiff and brittle. To improve elasticity of scaffold, TPU was added to natural fibers, such as collagen and chitosan. TPU proportion of 10%, 20%, 25% and 30% were investigated to determine the optimal component ratio. According to our observation, blended fibrous scaffolds with TPU proportion lower than 20% would be easily broken when squeezed or stretched, making them too fragile for tubular applications. Therefore, TPU proportion should not be set below 25% otherwise the elongation at break of crosslinked scaffolds could not exceed 10% and the scaffolds were too fragile to meet the flexibility requirements of tubular grafts.

The tensile strength of the aligned nanofibrous scaffolds showed significant differences between parallel (14.93 ± 0.59 MPa) and perpendicular (5.04 ± 0.95 MPa) directions. Moreover, comparison of elongation at break between scaffolds of parallel and perpendicular alignment showed an even sharper difference ($58.92 \pm 15.46\%$ as opposed to $8.20 \pm 0.84\%$).

As described before, GTA crosslinking had a negative effect on elongation at break, whereas at parallel direction crosslinked scaffolds boasted better elasticity than non-crosslinked ones. While

Table 1
Pore diameter of randomly oriented and aligned collagen–chitosan–TPU nanofibrous scaffolds.

Collagen–chitosan–TPU nanofibrous scaffolds	Specimen thickness (mm)	Mean flow pore diameter ± SD (μm)	Largest pore diameter (μm)	Smallest pore diameter (μm)
Aligned				
Non-crosslinked	0.108	0.2562 ± 0.0872	0.6032	0.1796
Crosslinked	0.088	0.1002 ± 0.0197	0.1743	0.0711
Randomly oriented				
Non-crosslinked	0.115	0.3745 ± 0.1084	0.8119	0.279
Crosslinked	0.105	0.2447 ± 0.1414	0.3185	0.0823

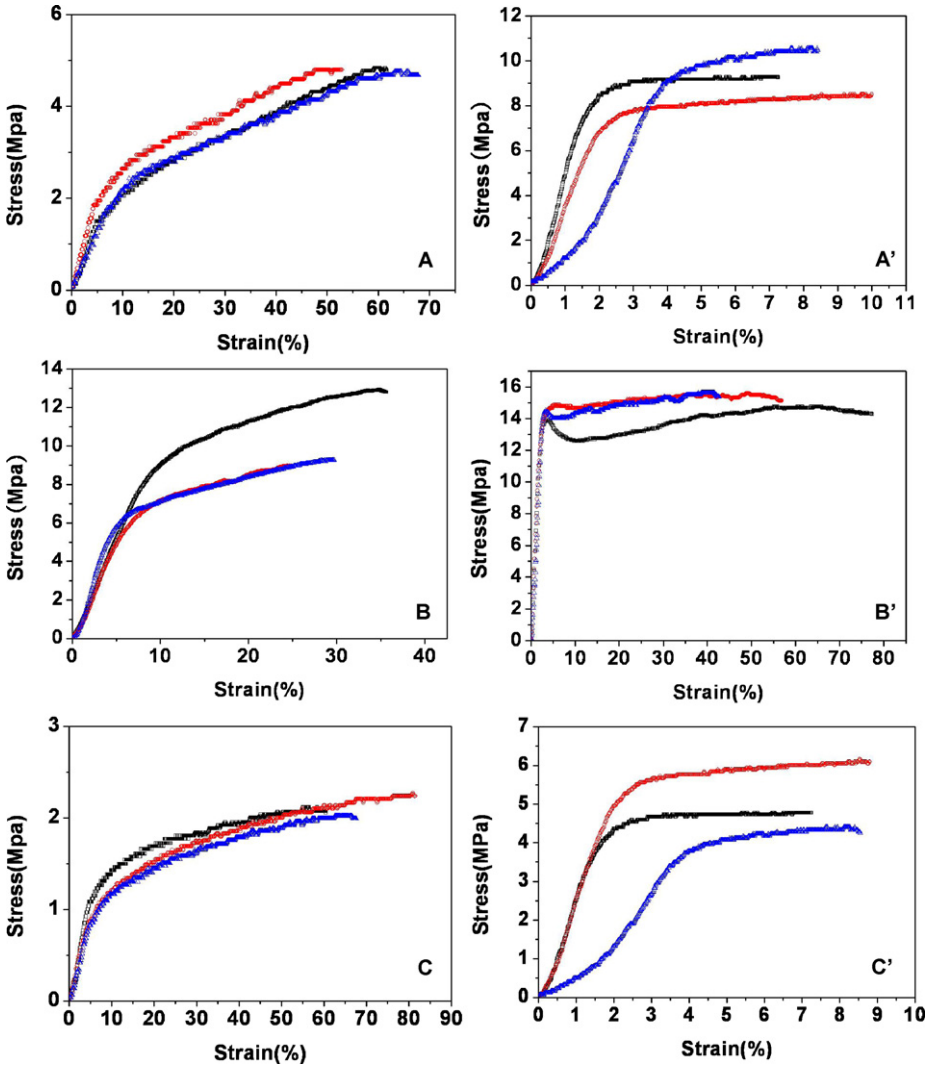

Fig. 6. Stress–strain curves of collagen–chitosan–TPU scaffolds. (A) and (A′) randomly oriented nanofibrous scaffolds before and after crosslinking; (B) and (B′) aligned nanofibrous scaffolds at parallel direction before and after crosslinking; (C) and (C′) aligned nanofibrous scaffolds at perpendicular direction before and after crosslinking.

aligned samples (crosslinked) were stretched along the direction of fiber orientation, there exists a unique fracture behavior. Fig. 7 shows that both random and aligned samples started to rupture with a small crack when tensile strength reached peak value, however, instead of extending to neighbouring fibers, the cracks on parallel samples preferred to move along the direction of fiber orientation and a small part of the sample was torn before the breakage of the entire sample. Thus, the sample had a higher percentage reading for elongation at break, and could be stretched further. This fracture behavior could also be reflected from Fig. 6B′, where a yielding point was formed on every stress–strain curve. The underlying mechanism was that unlike conventional fractures, when aligned fibers were stretched along parallel direction and formed a small crack, 'slippage' occurred amongst fibers; the paralleled fibers tended to slit along fiber orientation direction, and fractures were reduced as a result. Similar phenomenon did not occur on non-crosslinked samples, indicating that prior to GTA vapor crosslinking, scaffolds were quite sticky with a much larger sliding friction force between neighbouring fibers. Therefore, the crosslinked collagen–chitosan–TPU aligned nanofibrous scaffolds,

Table 2
Mechanical properties of randomly oriented and aligned collagen–chitosan–TPU nanofibrous scaffolds before and after GTA crosslinking. Data are representatives of 6 independent experiments and all the data are used as means ± SD.

Collagen–chitosan–TPU nanofibrous scaffolds	Average specimen thickness (mm)	Average elongation at break (%)	Average tensile strength (MPa)
Randomly oriented			
Non-crosslinked	0.086 ± 0.008	61.30 ± 3.88	4.64 ± 0.23
Crosslinked	0.082 ± 0.005	9.87 ± 1.77	9.38 ± 1.04
Aligned (parallel)			
Non-crosslinked	0.080 ± 0.006	30.10 ± 5.31	10.32 ± 1.73
Crosslinked	0.079 ± 0.006	58.92 ± 15.46	14.93 ± 0.59
Aligned (perpendicular)			
Non-crosslinked	0.084 ± 0.009	69.85 ± 8.67	2.11 ± 0.12
Crosslinked	0.081 ± 0.004	8.20 ± 0.84	5.04 ± 0.95

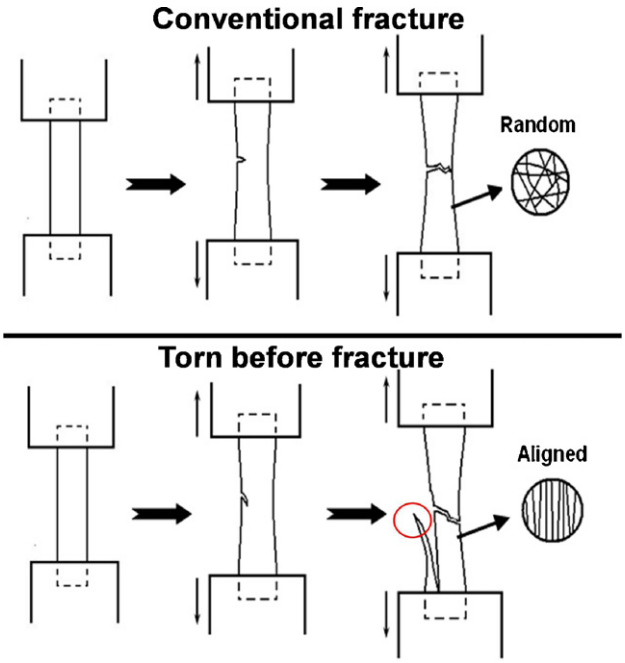

Fig. 7. Illustration of conventional fracture and slippage along parallel direction.

which possessed good mechanical properties at parallel direction, were more suitable for the fabrication of tissue engineered nerve conduits.

3.5. Viability of PIECs and SCs on nanofibrous scaffolds

For tissue engineered scaffolds, surface chemistry and topography are major factors in regulating cell behavior, including cell adhesion, cell proliferation, cell differentiation and cell morphology [27]. Proliferation of PIECs and SCs cultured on different electrospun scaffolds was determined by MTT assay after culturing for 1, 3, 5, and 7 days and the results are shown in Fig. 8. For the proliferation of PIECs, both randomly oriented and aligned electrospun scaffolds had better cell viability in comparison with TCP. Meanwhile, the proliferation rate of randomly oriented and aligned scaffolds showed no significant difference, indicating that the viability of PIECs was not affected by fiber orientation and pore size. As for SCs, random nanofibers showed a cell proliferation of approximately 25% higher than that of aligned fibers from day 3 to day 7. It is possible that compared with SCs, PIECs grow faster regardless of the substrate morphology, and SCs seem to be more sensitive to the environment, which is to say that if surface morphology of the growing media is altered, SCs viability can be easily influenced with a preference to random fibrous scaffolds. In nerve repair, this shortage might be solved by allowing for longer culturing duration for SCs.

Cell morphology and its relation with randomly oriented and aligned electrospun scaffolds were studied in vitro for 3 days. The resulting SEM images are listed in Fig. 9 and H&E staining micrographs are listed in Fig. 10 as complements. PIECs showed normal cell morphology on random fibers (Figs. 9A and 10A) whereas on aligned fibers, they seemed to show a slightly oriented arrangement. We can see from Fig. 9A′ that single PIEC was still able to retain its typical cell morphology while the orientation degree was comparatively lower. Compared to PIECs, SCs are more responsive to the seeding matrix. As can be seen from Fig. 9C and D, cells on random oriented nanofibrous scaffolds were mostly round whereas they exhibited spindle-shaped morphology on aligned fibers. Similar phenomenon could also be found on the H&E staining images (Fig. 10B and B′). Unfortunately, although cell morphology could be directly identified on the H&E staining pictures, fiber profiles are not clear. This is because once stained, colors on the protein collagen are very difficult to be thoroughly washed away. However, it is clear from the SEM pictures that fibers morphology and diameter were not obviously influenced by GTA crosslinking, indicating that a GTA crosslinking period of 48 h could ensure the electrospun fibers to maintain their original morphologies in culture medium.

3.6. Preparation of tubular scaffolds

The aim of this study is to design a novel kind of scaffolds for blood vessel and nerve repairs, so it is necessary to find a balance between biocompatibility and mechanical strength. As is described above, collagen and chitosan were electrospun to mimic the protein–polysaccharide based structure of native ECM while the addition of TPU could support the scaffolds with enough flexibility.

Randomly oriented nanofibrous vascular grafts were obtained by directly electrospinning the fibers on a 3 mm diameter steel cudgel with a low rotating speed (250–500 r/min). To make nerve conduits with aligned fibers, the membranes were cut into strips with fixed-size and then sutured into tubular shapes with a diameter of 1 mm. All the relevant pictures are shown in Fig. 11. From the bottom picture of Fig. 11 we can see that the tubular grafts made of collagen–chitosan–TPU nanofibers have good flexibility, which guaranteed the application of these grafts in vascular repair and nerve regeneration. However, as one major purpose of electrospinning is to create seamless structures, the suturing method used in this study seems to be an imperfect method. Therefore, the method to fabricate seamless electrospun aligned fibrous tubes should be explored.

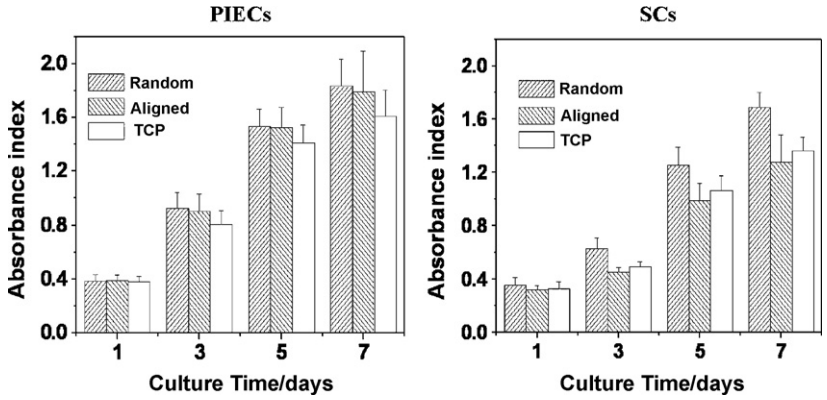

Fig. 8. Comparison of PIECs and SCs proliferation on randomly oriented and aligned collagen–chitosan–TPU nanofibrous scaffolds and TCP.

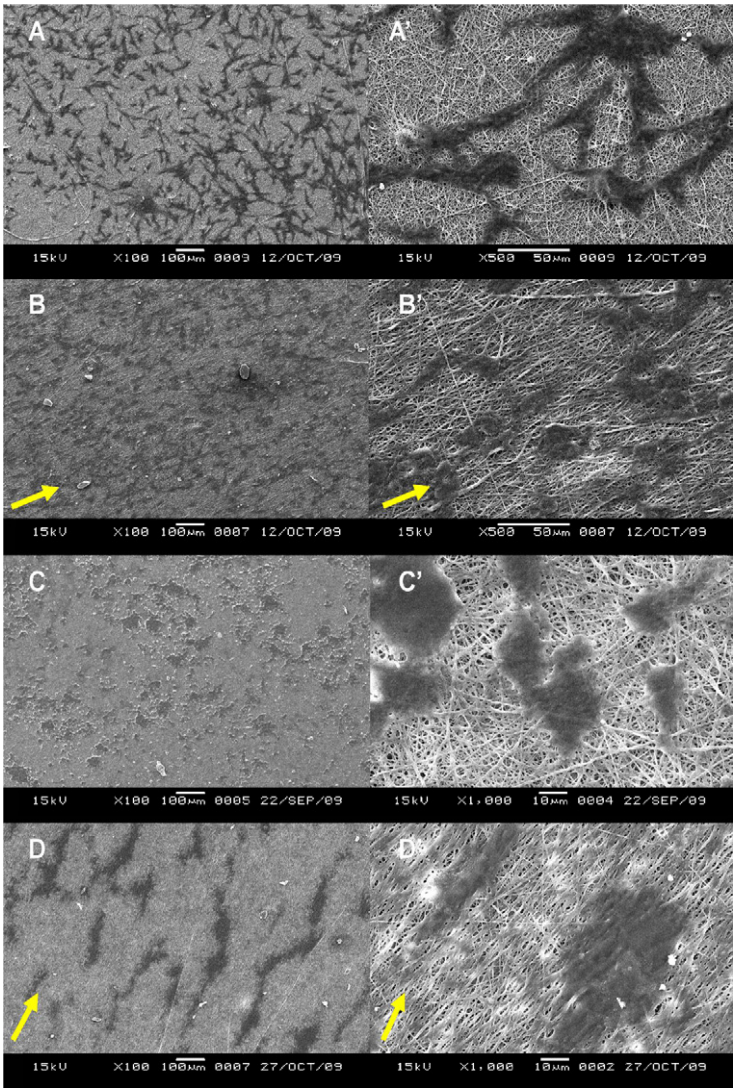

Fig. 9. SEM micrographs of PIECs and SCs on nanofibrous scaffolds after day 3 of cell culture: (A) and (A′) PIECs on randomly oriented nanofibers; (B) and (B′) PIECs on aligned nanofibers; (C) and (C′) SCs on randomly oriented nanofibers; (D) and (D′) SCs on aligned nanofibers.

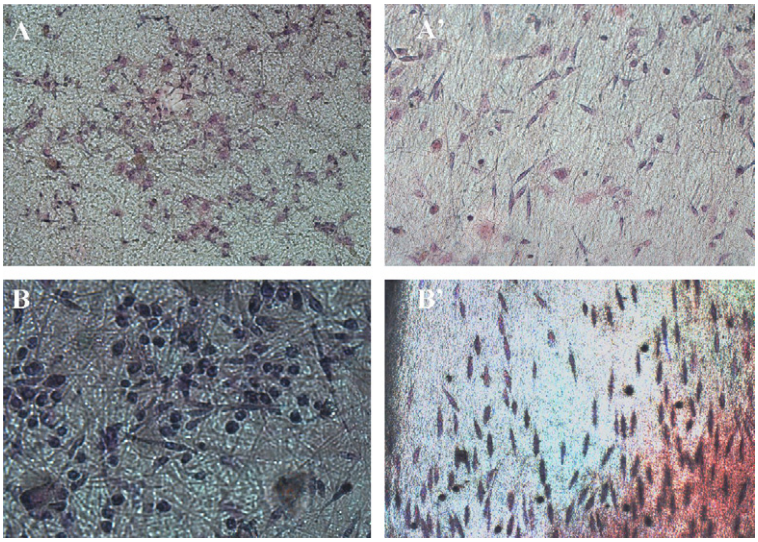

Fig. 10. H&E staining images of PIECs and SCs on nanofibrous scaffolds after day 3 of cell culture: (A) PIECs on randomly oriented nanofibers; (A′) PIECs on aligned nanofibers; (B) SCs on randomly oriented nanofibers; and (B′) SCs on aligned nanofibers.

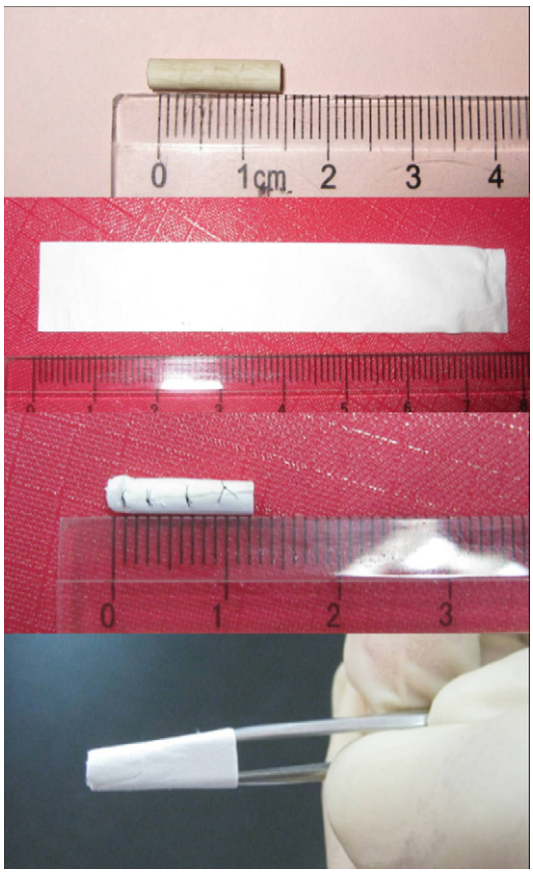

Fig. 11. Macrographic image of small diameter electrospun vascular graft and nerve conduit.

4. Conclusion

In this study, a balance between biocompatibility and mechanical properties was found by adjusting the proportion of natural and synthetic materials with the aim to produce a novel type of nanofibrous scaffolds that is suitable for blood vessel and nerve repairs. Collagen and chitosan were selected to biomimic the native ECM while TPU was added to improve mechanical properties of the scaffold. Scaffold characterization and cell viability study demonstrated that the three-material based scaffolds had a profound application potential in blood vessel repair and nerve regeneration. The next step will be focused on the in vivo study of these electrospun vascular grafts and nerve conduits.

Acknowledgements

This research was supported by National High Technology Research and Development Program (863 Program, 2008AA03Z305), "111 Project" Biomedical Textile Materials Science and Technology (B07024-SP0912) and Shanghai Unilever Research and Development Fund (08520750100).

References

[1] B.W. Tillman, et al., The in vivo stability of electrospun polycaprolactone–collagen scaffolds in vascular reconstruction, Biomaterials 30 (4) (2009) 583–588.
[2] S. Wang, et al., Acceleration effect of basic fibroblast growth factor on the regeneration of peripheral nerve through a 15-mm gap, Journal of Biomedical Materials Research – Part A 66 (3) (2003) 522–531.
[3] P.C. Francel, et al., Regeneration of rat sciatic nerve across a LactoSorb bioresorbable conduit with interposed short-segment nerve grafts, Journal of Neurosurgery 99 (3) (2003) 549–554.
[4] X. Wang, P. Lin, Q. Yao, C. Chen, Development of small-diameter vascular grafts, World Journal of Surgery 31 (4) (2007) 682–689.
[5] R. Langer, J.P. Vacanti, Tissue engineering, Science 260 (5110) (1993) 920–926.
[6] B. Alberts, et al., Essential Cell Biology, Garland Science, New York/London, 2004.
[7] G.A. Di Lullo, et al., Mapping the ligand-binding sites and disease-associated mutations on the most abundant protein in the human, type I collagen, Journal of Biological Chemistry 277 (6) (2002) 4223–4231.
[8] Z.G. Chen, et al., Electrospun collagen–chitosan nanofiber: a biomimetic extracellular matrix for endothelial cell and smooth muscle cell, Acta Biomaterialia 6 (2) (2010) 372–382.
[9] R. Chen, et al., Preparation and characterization of coaxial electrospun thermoplastic polyurethane/collagen compound nanofibers for tissue engineering applications, Colloids and Surfaces B: Biointerfaces 79 (2) (2010) 315–325.
[10] A. Sionkowska, et al., Molecular interactions in collagen and chitosan blends, Biomaterials 25 (5) (2004) 795–801.
[11] A. Pedicini, R.J. Farris, Mechanical behavior of electrospun polyurethane, Polymer 44 (22) (2003) 6857–6862.
[12] S.H. Lim, H.Q. Mao, Electrospun scaffolds for stem cell engineering, Advanced Drug Delivery Reviews 61 (12) (2009) 1084–1096.
[13] R. Murugan, S. Ramakrishna, Nano-featured scaffolds for tissue engineering: a review of spinning methodologies, Tissue Engineering 12 (3) (2006) 435–447.
[14] W.J. Li, et al., Electrospun nanofibrous structure: a novel scaffold for tissue engineering, Journal of Biomedical Materials Research 60 (4) (2002) 613–621.
[15] Z.M. Huang, Y.Z. Zhang, M. Kotaki, S. Ramakrishna, A review on polymer nanofibers by electrospinning and their applications in nanocomposites, Composites Science and Technology 63 (15) (2003) 2223–2253.
[16] T. Courtney, et al., Design and analysis of tissue engineering scaffolds that mimic soft tissue mechanical anisotropy, Biomaterials 27 (19) (2006) 3631–3638.
[17] C.A. Bashur, L.A. Dahlgren, A.S. Goldstein, Effect of fiber diameter and orientation on fibroblast morphology and proliferation on electrospun poly(D, L-lactic-co-glycolic acid) meshes, Biomaterials 27 (33) (2006) 5681–5688.
[18] M.V. Jose, et al., Aligned PLGA/HA nanofibrous nanocomposite scaffolds for bone tissue engineering, Acta Biomaterialia 5 (1) (2009) 305–315.
[19] Z. Chen, X. Mo, F. Qing, Electrospinning of collagen–chitosan complex, Materials Letters 61 (16) (2007) 3490–3494.
[20] Z.M. Huang, et al., Fabrication of a new composite orthodontic archwire and validation by a bridging micromechanics model, Biomaterials 24 (17) (2003) 2941–2953.
[21] S.Y. Chew, R. Mi, A. Hoke, K.W. Leong, Aligned protein–polymer composite fibers enhance nerve regeneration: a potential tissue-engineering platform, Advanced Functional Materials 17 (8) (2007) 1288–1296.
[22] H.B. Wang, et al., Creation of highly aligned electrospun poly-L-lactic acid fibers for nerve regeneration applications, Journal of Neural Engineering 6 (1) (2009).
[23] E. Schnell, et al., Guidance of glial cell migration and axonal growth on electrospun nanofibers of poly-ε-caprolactone and a collagen/poly-ε-caprolactone blend, Biomaterials 28 (19) (2007) 3012–3025.
[24] C.H. Lee, et al., Nanofiber alignment and direction of mechanical strain affect the ECM production of human ACL fibroblast, Biomaterials 26 (11) (2005) 1261–1270.
[25] C.E. Ayres, et al., Measuring fiber alignment in electrospun scaffolds: a user's guide to the 2D fast Fourier transform approach, Journal of Biomaterials Science, Polymer Edition 19 (5) (2008) 603–621.
[26] D.I. Zeugolis, et al., Electro-spinning of pure collagen nano-fibres – just an expensive way to make gelatin? Biomaterials 29 (15) (2008) 2293–2305.
[27] M.M. Stevens, J.H. George, Exploring and engineering the cell surface interface, Science 310 (5751) (2005) 1135–1138.